

Monitoring of Homogenization and Analysis of Nanoscale Structure in a Butadiene–Acrylonitrile Copolymer/Poly(vinyl chloride) Blend[†]

Seung-Yeop Kwak* and Nobuyuki Nakajima

Institute of Polymer Engineering, The University of Akron, Akron, Ohio 44325

Received December 18, 1995; Revised Manuscript Received April 23, 1996[®]

ABSTRACT: The progress of homogenization in the mechanical blending of a butadiene–acrylonitrile copolymer (NBR) and a poly(vinyl chloride) (PVC) was observed with scanning and transmission electron microscopes. The significant events of the microscopic examinations were as follows: (i) NBR formed a continuous and PVC a dispersed phase. (ii) The skins of PVC grains (100–150 μm) were removed first, and the grains were broken into agglomerates ($\sim 10\ \mu\text{m}$). (iii) The agglomerates were disintegrated stepwise into primary particles ($\sim 1\ \mu\text{m}$), domains ($\sim 0.1\ \mu\text{m}$), and eventually the nodular particles of the size between domains and microdomains ($\sim 10\ \text{nm}$). The electron microscopic visualizations, together with the material behavior expressed in terms of the internal mixer geometry and the viscoelastic properties during mixing action, suggest a schematic model for the homogenization mechanism. The microphase structure of the finished blend was characterized by cross-polarization/magic angle spinning (CP/MAS) ^{13}C NMR spectroscopy. Analyses of $T_{1\rho}$ spin–lattice relaxation for specific carbons permitted a precise identification of the microstructures. Double-component resolution of the magnetization decay confirmed a coexistence of a mixed phase and two microseparated phases, the latter corresponding to an unmixed NBR phase and PVC microcrystallites. From the $T_{1\rho}$ relaxation times, the sizes of the microphases were estimated to be in the nanoscale.

Introduction

Blends of butadiene–acrylonitrile copolymer (NBR) and poly(vinyl chloride) (PVC) have been of commercial success because they possess a number of improved end properties over the individual component polymers.^{1,2} For practical reasons, the blend is usually produced by mechanical mixing, where a level of homogeneity is adjusted for the intended application. Recognizing that the mechanical mixing requires high energy, monitoring the progress of mixing is of first importance for acquiring information on the efficient operation with satisfactory quality of the mix. Because the morphology developed during mixing intimately relates to the solid-state phase structure and properties, elucidation of the homogenization mechanism how this morphology evolves is of critical importance in such a blend system.^{3,4} Furthermore, knowledge of the homogenization mechanism would be useful for the design of processing equipment with improved mixing performance.^{3,4} Then, the analysis of the phase structure in the finished blend is of another importance because it governs the physical/mechanical properties in its end use.

In this study, a model mixing of an equal amount (1:1 mass ratio) of an NBR containing 30% acrylonitrile and a suspension-polymerized PVC is conducted in a batch internal mixer, and the progress of homogenization is examined with a scanning and a transmission electron microscope. The suspension PVC, as schematically illustrated in Figure 1, is a powder of about 100–150 μm , called grains, consisting of skin and tight agglomerates ($\sim 10\ \mu\text{m}$); the agglomerate is composed of primary particles ($\sim 1\ \mu\text{m}$) which in turn consist of domains ($\sim 0.1\ \mu\text{m}$); the domain is made up of microdomains ($\sim 10\ \text{nm}$) which are held internally by microcrystallites acting as

physical cross-links which contribute to the strength of PVC.^{3–6}

For identifying and analyzing the microphase structure of a particular blend system, various techniques have been employed, and their applicability, the inherent resolution, and the information that they yield are known to differ widely.^{7–9} For example, a presence of the microstructure in the NBR/PVC blend may be examined by the temperature dependence of frequency-swept dynamic mechanical properties; the information obtained is indirect and qualitative. More sensitive and quantitative characterization of the microstructure on a nanoscale level may be performed by the nuclear magnetic resonance (NMR) spectroscopy. In this study, ^{13}C NMR measurements of proton spin–lattice relaxation time in the rotating frame, $T_{1\rho}$, are performed with a cross-polarization/magic angle spinning (CP/MAS).

Experimental Section

Materials, Mixing Procedures, and Sample Preparation. NBR was HYCAR VT 380 (Zeon Chemicals) containing 30% acrylonitrile; its glass transition temperature (T_g) is about $-28\ ^\circ\text{C}$. PVC resin was Geon 103 EP F-76 (Geon Co.) with number-average molecular weight 44 000 and weight-average molecular weight 89 000.¹⁰

NBR, 50% by weight, and PVC, 50% by weight with 1% thermal stabilizer (Therm-Chek 1872 from Ferro Corp.), were mixed in a nonintermeshing, counterrotating two-wing rotor internal mixer (1.57 L Farrel Banbury mixer). The rotor speed was 80 rpm, and the fill factor was about 0.7. Before mixing, NBR was first masticated at room temperature for 30 s and then the rotor was stopped. At this stage, the built-in thermometer of the mixer indicated $65\ ^\circ\text{C}$. PVC was charged in the mixer, the ram was lowered, and the rotor was restarted. From this moment, the mixing time was measured. At various intermediate stages during the progress of mixing, the machine was stopped and samples were removed for the microscopic examination. The temperature during mixing increased, reaching a maximum ($165\ ^\circ\text{C}$) after 150 s and then decreased slightly by about 5 deg to a constant value.

After 450 s, the mixing was considered to be completed and the blend was sheeted out through a two-roll mill. The sheets

* To whom correspondence should be addressed at the Division of Polymer Research, Korea Institute of Science and Technology (KIST), P.O. Box 131, Cheongryang, Seoul 130-650, Korea.

[†] Presented at the Eleventh Annual Meeting of the Polymer Processing Society, Seoul, Korea, March 25–27, 1995.

[®] Abstract published in *Advance ACS Abstracts*, July 1, 1996.

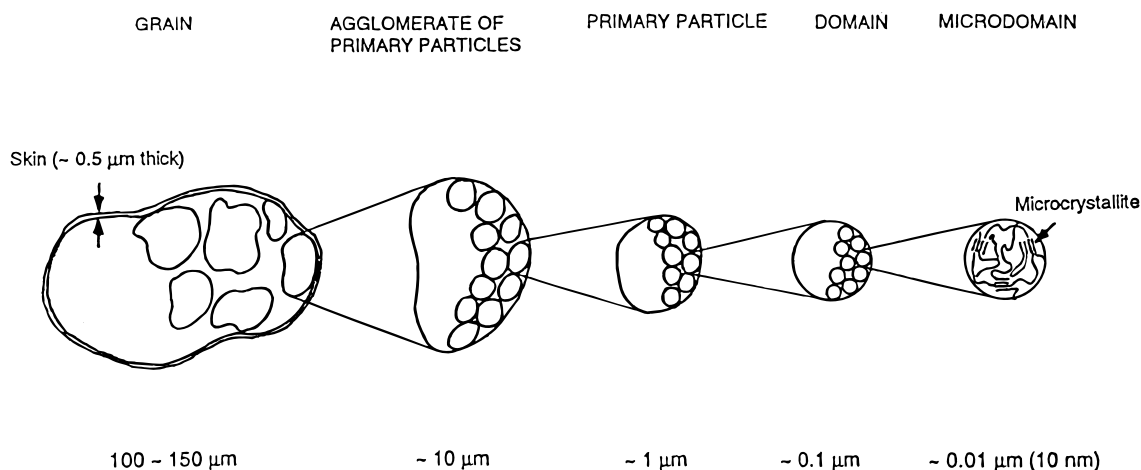


Figure 1. Structural hierarchy of suspension poly(vinyl chloride) (PVC).

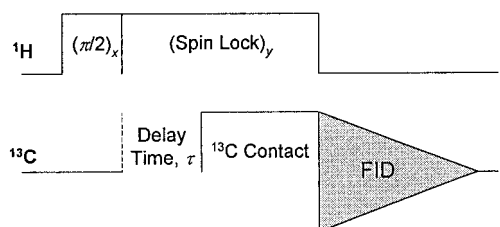


Figure 2. Cross-polarization (CP) pulse sequence to determine $T_{1\rho}$ relaxation times under the Hartmann-Hahn matching condition.

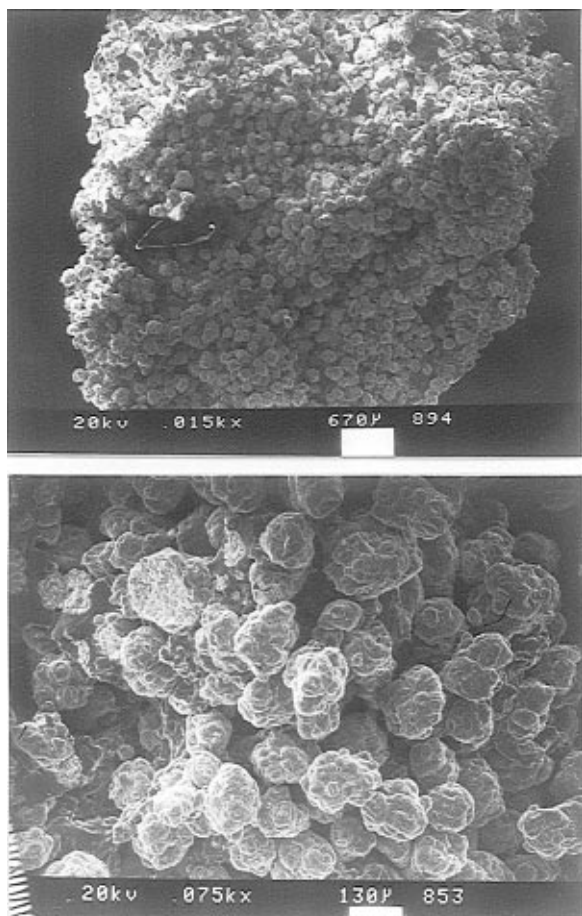


Figure 3. Scanning electron micrographs of the NBR/PVC mixture at a mixing time of 30 s, and two magnifications.

were compression molded, cooled, and chopped into small pieces of about 1 mm × 1 mm for the NMR experiments.

Electron Microscopy. An ISI SX-40 scanning electron microscope (SEM) and a JEOL 100 CX-II transmission electron

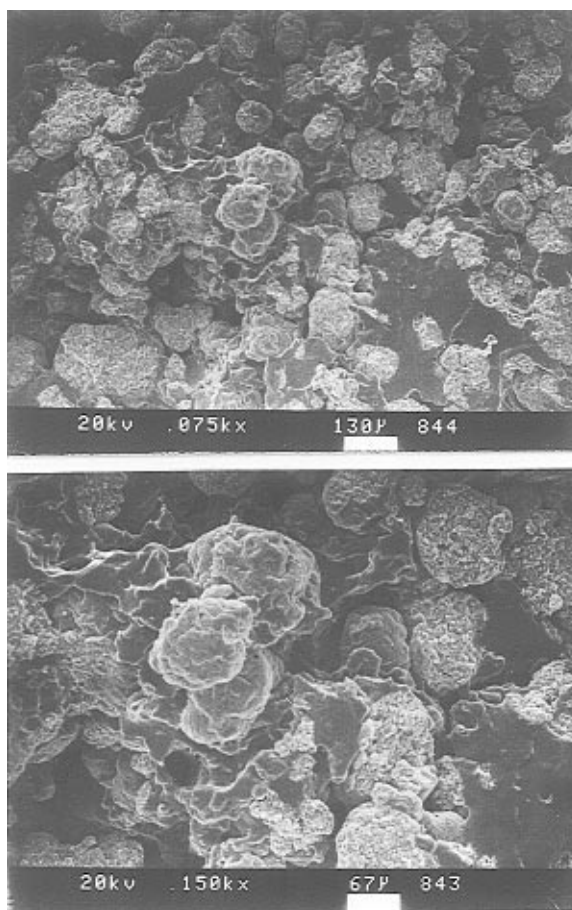


Figure 4. Scanning electron micrographs of the NBR/PVC mixture at a mixing time of 50 s, and two magnifications.

microscope (TEM) were used. For the SEM observation, the samples removed from the mixer at intermediate stages during mixing were cut into appropriate size, immersed in liquid nitrogen, and freeze-fractured. The fracture surfaces were inspected after being sputter-coated with silver. For the TEM observation, approximately 1 mm thick sheets were cut from the mixture taken out at the mixing time of 150 s. They were exposed to the vapor of osmium tetroxide (OsO_4) at room temperature for about 5 days and then dried at room temperature under vacuum for 20 min. By this procedure, the NBR phase was selectively stained to a depth of several micrometers from the surface of the sheet. Ultrathin sections were cut parallel to the surface of the sheet by a ultramicrotome and examined with TEM.

CP/MAS ^{13}C NMR Spectroscopy. In the CP/MAS ^{13}C NMR, the naturally rare ^{13}C spins are polarized through the dipolar coupling with the abundant ^1H spins and the magnetization of the ^1H is transferred to the ^{13}C . This brings about

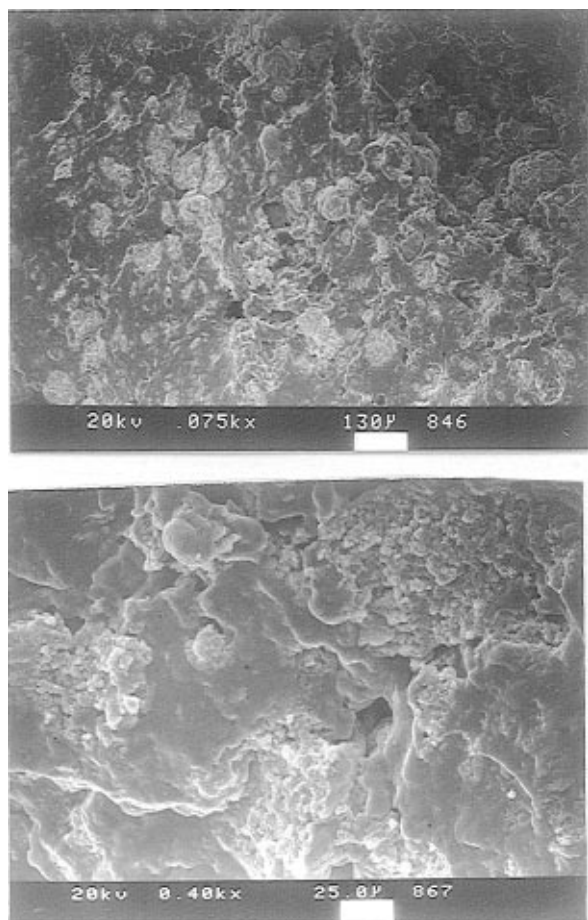


Figure 5. Scanning electron micrographs of the NBR/PVC mixture at a mixing time of 70 s, and two magnifications.

significant enhancement of ^{13}C signal intensity and reduction in data acquisition time.¹¹ Moreover, the MAS contributes to removal of the heteronuclear dipole–dipole interactions and the chemical shift anisotropy, thereby narrowing the line widths of the spectrum; the resonance of carbons attached to the different nuclear environments can be resolved.¹²

The NMR experiments were performed with a Chemagnetic CMX-300 spectrometer (299.6 MHz for ^1H) equipped with a magic angle spinning probe. The sample was packed in zirconia rotors with Kel-F end caps and spun at the rate of about 3.5 kHz. A ^1H 90° pulse width of 4.25 μs was employed with *ca.* 5000 FID signal accumulations. $T_{1\rho}$ spin–lattice relaxation times were measured by monitoring the decay of specific carbon peak intensities after ^1H spin-lock– τ pulse sequence prior to cross-polarization (CP), Figure 2. The CP Hartmann–Hahn contact time was 1 ms.

Results and Discussion

Figures 3–7 show the SEM results of the homogenization up to a mixing period of 130 s; the scale bar is shown at the bottom right of each micrograph. The sample at a mixing time of 30 s (Figure 3) contains a small amount of free-flowing PVC particles. Most particles adhere to the rubber, covering its surface. The PVC particles are intact; that is, the skins of individual particles still cover unbroken particles. At a mixing time of 50 s (Figure 4), very few free-flowing PVC particles exist. The skins of PVC particles are peeled off, and some particles are broken. The skinless particles become incorporated into the rubber matrix, but the particles with their skin remaining do not. At a mixing time of 70 s (Figure 5), all PVC particles have their skins removed and are incorporated into the rubber; the rubber becomes the continuous phase. With 90 s mixing (Figure 6), the skinless particles are broken

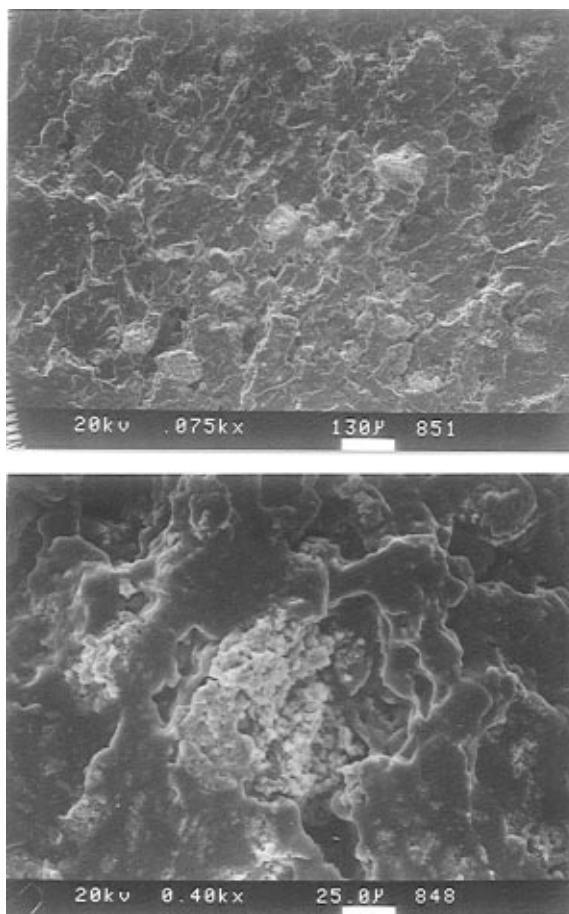


Figure 6. Scanning electron micrographs of the NBR/PVC mixture at a mixing time of 90 s, and two magnifications.

down into smaller particles, some of them reaching the size of the agglomerates ($\sim 10\ \mu\text{m}$). With further mixing, 110 s (Figure 7a), a large number of PVC agglomerates are shown to have been broken down into the primary particles ($\sim 1\ \mu\text{m}$). Then, the breakdown process becomes more severe and at 130 s (Figure 7b) the primary particles disintegrate into the domains ($\sim 0.1\ \mu\text{m}$), finely dispersed throughout the rubber matrix.

These SEM visualizations, in conjunction with the geometry of the internal mixer and the deformation behavior of the materials during the mixing action, enable us to construct a model for the homogenization mechanism. Traditionally, the rubber in the mixing condition has been regarded as a fluid¹⁵ and the material behavior has been represented by a steady-state flow.¹⁶ However, the steady state is nearly impossible in the internal mixer because the width of the channel where the rubber is transported is changing with time and a large deformation, often exceeding the ultimate stress, is usually involved. Furthermore, rubbers at an optimum mixing condition are in the elastic state (refer to Tokita–White region II^{17,18}) rather than the flow state. Therefore, the material behavior in the elastic state is more appropriately described by deformation rather than flow. As described in the Experimental Section, NBR was first masticated for 30 s before mixing with PVC, and the temperature of NBR reached 65 °C. Figure 8a shows the viscoelastic profile of NBR at an angular frequency range of 10^{-2} – 10^2 rad/s and at 65 °C. Considering that the rpm of the rotor was 80, this value approximately corresponds to the angular frequency of *ca.* 8 rad/s ($80\ \text{rpm} \approx 1.3\ \text{s}^{-1} \approx 8\ \text{rad/s}$ by $\omega = 2\pi\nu$). At the angular frequency of 8 rad/s, NBR is in the rubbery elastic state at this temperature. Figure 8b represents the viscoelastic profile of NBR at a fixed

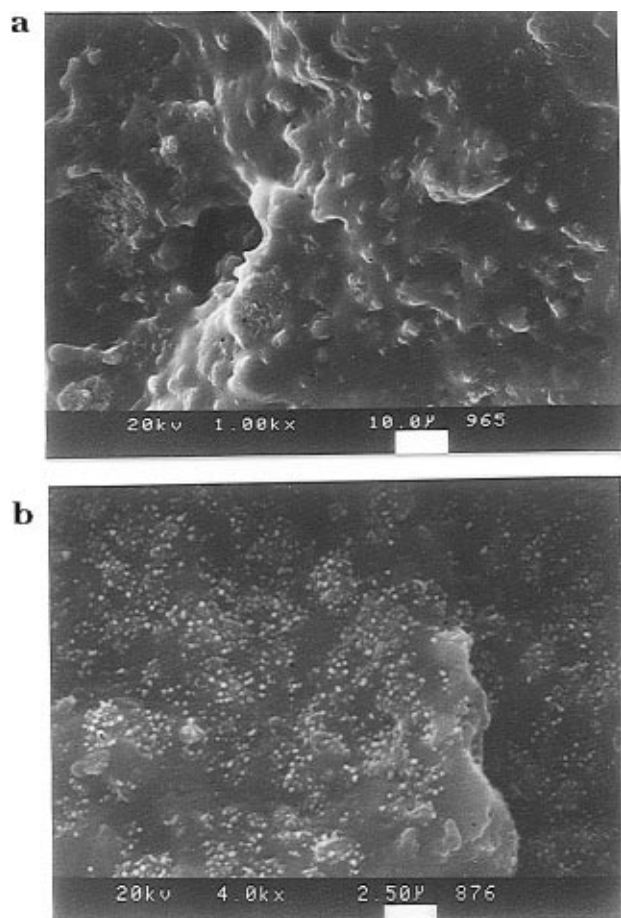


Figure 7. Scanning electron micrographs of the NBR/PVC mixture at mixing times of 110 s (a) and 130 s (b).

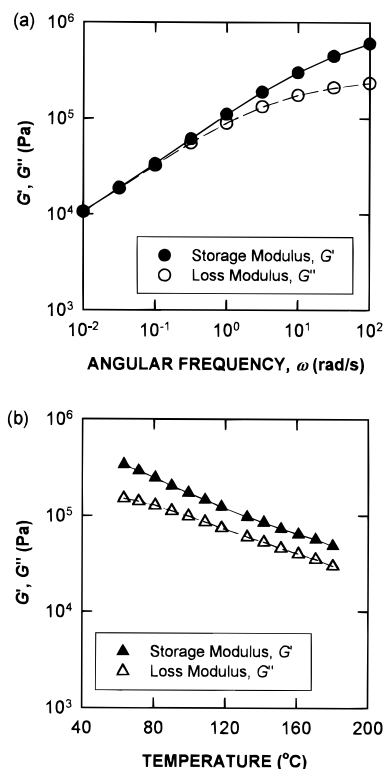


Figure 8. Storage modulus, G' , and loss modulus, G'' , of NBR as a function of angular frequency, ω , at 65 °C (a) and as a function of temperature at an oscillation frequency of 1.3 Hz (b).

frequency of oscillation of 1.3 Hz (≈ 8 rad/s) as a function of temperature. The frequency and the temperature range were selected to correspond to the rpm of the rotor

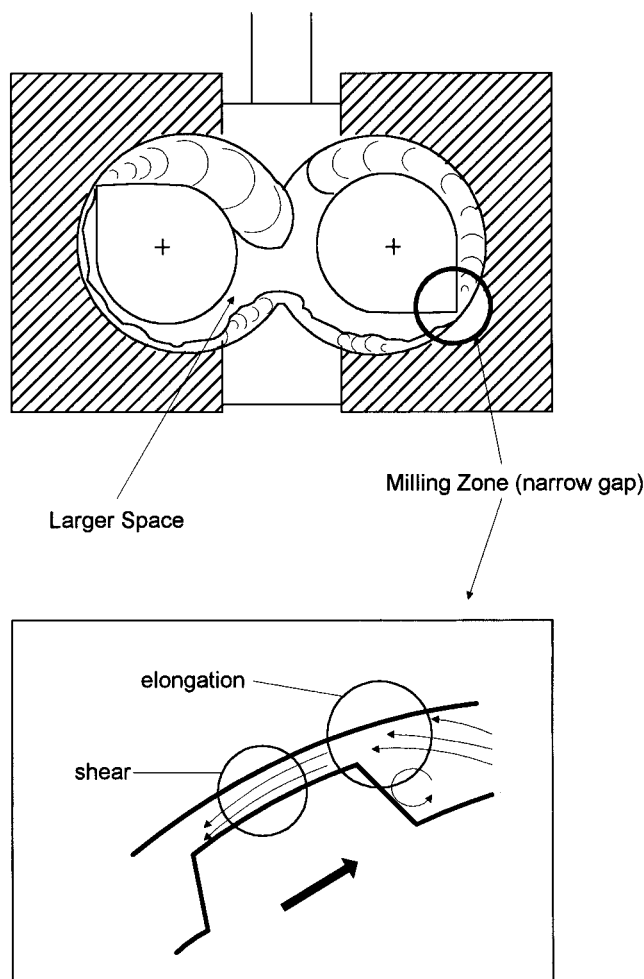


Figure 9. Schematic view of the deformation situation and material behavior in the internal mixer.

and that observed during mixing, respectively. NBR remains in the rubbery state throughout the temperature range of mixing with G' decreasing from $ca. 3.3 \times 10^5$ to 6.1×10^4 Pa, indicating that NBR behaves as a deformable solid during mixing.

As seen in Figure 9, there are two characteristic geometric features in the internal mixer: (i) a narrow gap, *i.e.*, milling zone, between rotor blades and the chamber wall and (ii) a larger space between two rotors. In the larger space zone, the material movement is in both axial and lateral directions, resulting in kneading, longitudinal cut-back, and lateral overlap.¹⁹ This zone provides mostly macroscopic homogenization because the deformation rate is relatively low. An effective mixing (dispersion) takes place primarily in the milling zone, where the deformational stress is highest. In the milling zone, the material is deformed from a larger to a smaller cross section, *i.e.*, elongational deformation.²⁰ The velocity difference between the blade surface and the chamber wall also creates shear deformation. Consequently, the material behavior in the internal mixer reflects a combination of elongational and shear deformation.

On the basis of the geometry and the material behavior in the mixer, the SEM morphologies presented in the mixing period of 130 s suggest a model for the initial mechanism of homogenization, as depicted in Figure 10. When NBR pieces pass through the milling zone, they experience a large deformation by shear as well as elongation, creating a high stress, and act as a medium to transfer the stress from the machine to the PVC particles. This process brings about peeling-off

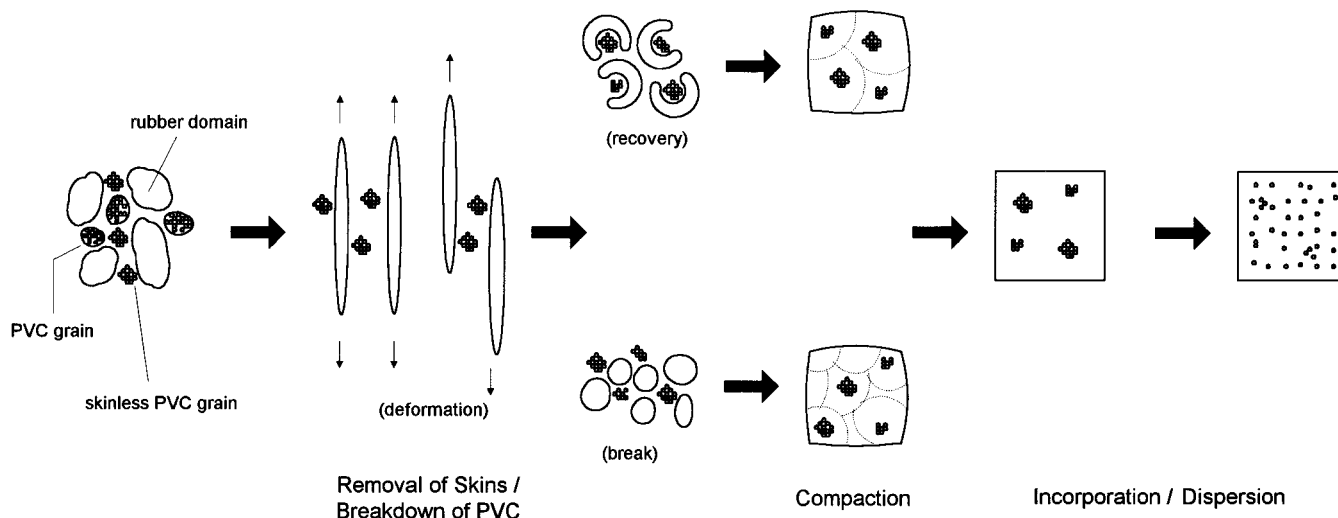


Figure 10. Proposed model for homogenization mechanisms involving skin removal and breakdown of PVC.

(removal) of the skins of PVC grains and also breakdown of the skinless PVC particles. The deformed rubber relaxes or breaks up, depending on whether the ultimate strain is reached, and then recovers its strain. Because of the compacting pressure, the skin-removed and disintegrated PVC particles are incorporated into the rubber phase. In the zones which have larger space than the milling zone, a simple mixing (*i.e.*, macroscopic homogenization) occurs and it makes the PVC particles move without changing their physical shape, resulting in an increase of the randomness of the spatial distribution and hence the entropy of the mix. This process may take place during the whole mixing cycle. As the mixing cycle repeats, the dispersion process results in subsequent breakdown of the PVC particles and progressive spreading of them.

When the mixing reaches 150 s, Figure 11a, the dark area is the rubber which is broken to the size of 0.1–0.5 μm diameter. In Figure 11b, a nodular structure of PVC of about 50 nm or somewhat larger is seen as a white area. The nodular structure is very similar to that observed by Cobboldo *et al.*,²¹ who first identified the presence of microdomains (in their case, the size was 10–20 nm) by examining the replicated surface of PVC with a TEM.

As the mixing proceeds further, whether the size of the PVC particles may be reduced to a smaller size or not is the objective of the following NMR study. Figure 12 shows CP/MAS ^{13}C NMR spectra of NBR, PVC, and the 50/50 blend. For NBR, the resonance peaks at 131 and 33 ppm are assigned to methine/cyanide (CH/CN) and methylene (CH_2) carbons, respectively. The two peaks at 57 and 46 ppm in the PVC spectrum are assigned to methine (CH) and methylene (CH_2) carbons, respectively. The spectrum of the blend is no more than a superposition of the spectra from NBR and PVC. Recognizing that the miscibility of NBR/PVC arises from a polar interaction between CN in NBR and Cl in PVC, the carbon peaks in the blend which we are concerned with are those for CH/CN and CH carbons. Variation in the resonance intensity ($M(\tau)$) for a specific carbon is obtained by the delayed-contact ^{13}C CP/MAS experiment (Figure 2) where various delay times (τ) are inserted between the $\pi/2$ pulse and the spin-locking pulse. Because the resonance intensity exponentially decays in concert with a proton magnetization with a time constant equal to the $T_{1\rho}$ by the following function,

$$M(\tau) = M_0 \exp(-\tau/T_{1\rho}) \quad (1)$$

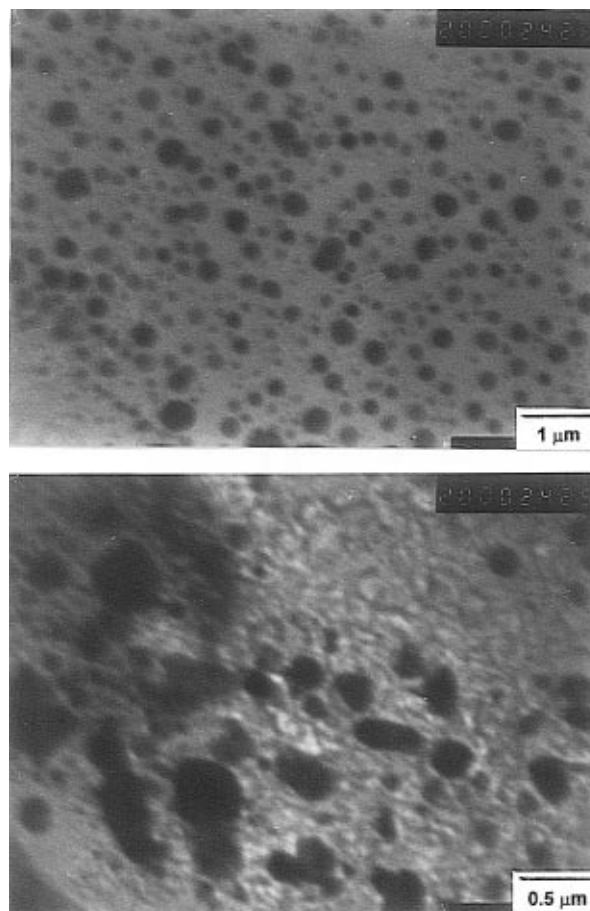


Figure 11. Transmission electron micrographs of the NBR/PVC mixture at a mixing time of 150 s, and two magnifications.

monitoring of the resonance decays provides the $T_{1\rho}$ determination.

Figure 13a expresses the $\ln M(\tau)/M_0$ vs τ plot for CH/CN of NBR alone and for CH of PVC alone, where the slope of the straight line determines the $T_{1\rho}$ relaxation time. PVC shows a double-component relaxation behavior, which indicates the presence of two phases. The short component with considerably shorter $T_{1\rho}$ (see Table 1) is for a more rigid phase, *i.e.*, microcrystallites, and the long component is for a more mobile phase, *i.e.*, amorphous chains. In contrast, NBR exhibits only one line and hence a single value of $T_{1\rho}$ (Table 1), indicating that the material is homogeneous. For the blend, Figure

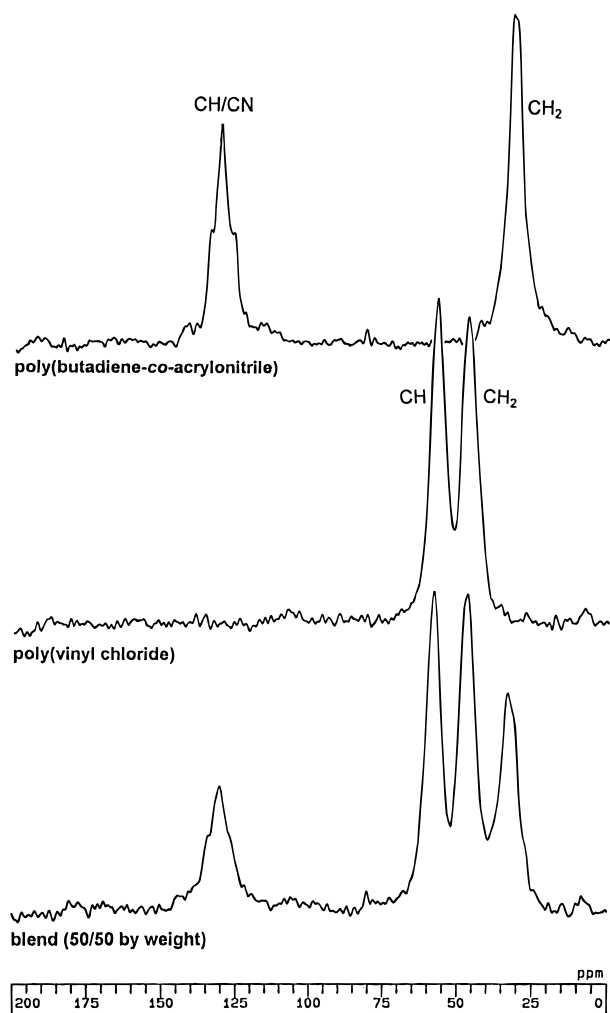


Figure 12. ^{13}C high-resolution CP/MAS spectra of NBR, PVC, and their 50/50 blend.

13b, double-component $T_{1\rho}$ relaxations were observed in both CH and CH/CN signals (the dotted lines in the figure are the same as those in Figure 13a). The longer time relaxations for CH/CN and CH are identical, implying that the protons of the constituent polymers relax at an average rate and are considered to be in the homogeneous environment,²² *i.e.*, a mixed phase. Two different $T_{1\rho}$'s from the short components indicate the presence of PVC microcrystallites and that of the unmixed NBR domains. The relaxation time of a distinguishable region provides an estimate of the diffusive path length and hence the characteristic size through the spin diffusion process.^{23–26} An approximate estimation of the domain size is given by relating the spin diffusion and the relaxation time, as follows:^{27,28}

$$\langle r \rangle = (6DT)^{1/2} \quad (2)$$

$\langle r \rangle$ is the average diffusive path length for the effective spin diffusion. D is the spin diffusion coefficient determined by the average proton-to-proton distance and the strength of the dipolar interaction; it has typically a fixed value of $10^{-12} \text{ cm}^2 \text{ s}^{-1}$. T is the characteristic time over which the spin diffusion proceeds, and here it is $T_{1\rho}$. It is noted that it is possible to estimate the maximum scale of the microheterogeneous domains with single-component decay and the minimum domain sizes with double-component decay through the above approximate equation.^{29,30} Thus, the minimum size of the microheterogeneous phases is estimated from the short-component $T_{1\rho}$ value of NBR to be $\sim 1.1 \text{ nm}$; this

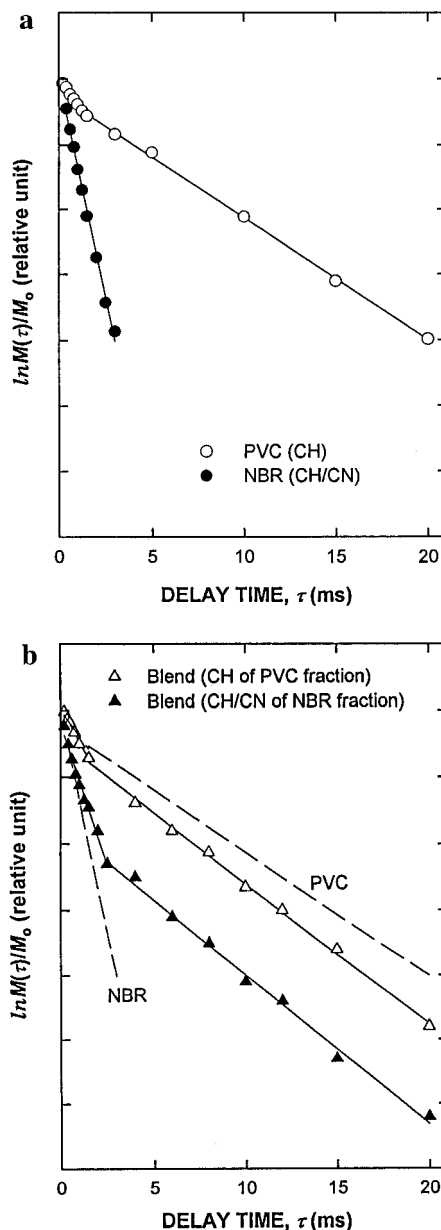


Figure 13. Rotating frame $T_{1\rho}$ decay of NBR and PVC in their respective unblended states (a) and the blended state (b).

Table 1. Proton $T_{1\rho}$ Relaxation Times of NBR, PVC, and the Blend

	$T_{1\rho}$ (ms)		
	carbon	short-component	long-component
NBR	CH/CN		1.52
PVC	CH	5.22	10.89
blend (50/50)	CH/CN	1.89	8.97
	CH	3.74	9.00

value is presumably for that of the concentration fluctuation of NBR rather than that of distinct domains. The maximum distance between the microseparated phases is approximately 2.3 nm.

Conclusions

The homogenization of mixing NBR and PVC in the initial period of 150 s proceeded as the skins of PVC grains were first peeled off and then the agglomerates were broken down to the primary particles ($\sim 1 \mu\text{m}$). Eventually, the particles reaching the size between the domains ($\sim 0.1 \mu\text{m}$) and the microdomains ($\sim 10 \text{ nm}$) were dispersed in the rubber. The rubber was also broken down to $0.1\text{--}0.5 \mu\text{m}$. A model for the homog-

enization mechanism was schematically proposed; the mechanisms of skin removal and PVC breakdown involved NBR as a deformable medium for the transfer of stress generated by the machine to PVC.

The blend after 450 s mixing was homogeneous in the microscopic examination but exhibited a double-component $T_{1\rho}$ relaxation behavior. This indicated the presence of microseparated phases, which were unmixed NBR and PVC microcrystallites. The minimum and maximum sizes of the microheterogeneous phases were estimated to be 1.1 and 2.3 nm, respectively.

References and Notes

- (1) Schwarz, H. F.; Bley, J. W. F. In *Advances in Polymer Blends and Alloys Technology*; Kohudic, M. A., Ed.; Technomic Publishing: Lancaster, PA, 1988; Vol. 1, Chapter 10.
- (2) Stockdale, M. K. *J. Vinyl Technol.* **1990**, *12*, 235.
- (3) Scott, C. E.; Macosko, C. W. *Polymer* **1995**, *36*, 461.
- (4) Plochocki, A. P.; Dagli, S. S.; Starita, J.; Curry, J. E. *J. Elastomer Plast.* **1986**, *18*, 256.
- (5) Geil, P. H. *J. Macromol. Sci.-Phys.* **1977**, *B14*, 171.
- (6) Davidson, J. A.; Gardner, K. L. *Encyclopedia of Chemical Technology*, 3rd ed.; Wiley & Sons: New York, 1983; Vol. 23.
- (7) Butters, G., Ed. *Particulate Nature of PVC*; Applied Science: London, 1982.
- (8) Munstedt, H. *J. Macromol. Sci.-Phys.*, **1977**, *B14*, 195.
- (9) Kaplan, D. S. *J. Appl. Polym. Sci.* **1976**, *20*, 2615.
- (10) Warfield, R. W.; Hartmann, B. *Polymer* **1980**, *21*, 31.
- (11) Bair, H. E.; Warren, P. C. *J. Macromol. Sci.-Phys.* **1981**, *B20*, 381.
- (12) Daniels, C. A.; Collins, E. A. *J. Macromol. Sci.-Phys.* **1974**, *B10*, 287.
- (13) Hartmann, S. R.; Hahn, E. L. *Phys. Rev.* **1962**, *128*, 2042.
- (14) Schaefer, J.; Stejskal, E. O. *J. Am. Chem. Soc.* **1976**, *98*, 1032.
- (15) McKelvey, J. M. *Polymer Processing*; Wiley & Sons: New York, 1962.
- (16) Palmgren, H. *Rubber Chem. Technol.* **1975**, *48*, 462.
- (17) Tokita, N.; White, J. L. *J. Appl. Polym. Sci.* **1966**, *10*, 1011.
- (18) White, J. L.; Tokita, N. *J. Appl. Polym. Sci.* **1968**, *12*, 1589.
- (19) *Understanding the Banbury Mixer*; Farrel Co.: Ansonia, CT 06401, 1968.
- (20) Nakajima, N.; Shida, M. *Trans. Soc. Rheol.* **1969**, *10*, 299.
- (21) Allsopp, M. W. in *Manufacture and Processing of PVC*; Burgess, R. H., Ed.; Macmillan: New York, 1982; Chapter 7 (private communication with A. J. Cobboldo).
- (22) Dickenson, L. C.; Yang, H.; Chu, C.-W.; Stein, R. S.; Chien, J. C. W. *Macromolecules* **1987**, *20*, 1757.
- (23) McBrierty, V. J.; Douglass, D. C. *J. Polym. Sci., Macromol. Rev.* **1981**, *16*, 295.
- (24) Linder, M.; Hendrichs, P. M.; Hewitt, J. M.; Macsa, P. J. *J. Chem. Phys.* **1985**, *82*, 1585.
- (25) Parmer, J. F.; Dickenson, L. C.; Chien, J. C. W.; Porter, R. S. *Macromolecules* **1989**, *22*, 1078.
- (26) Masson, J.-F.; Manley, R. St. J. *Macromolecules* **1991**, *24*, 6670.
- (27) McBrierty, V. J.; Douglass, D. C.; Kwei, T. K. *Macromolecules* **1978**, *11*, 1265.
- (28) McBrierty, V. J.; Douglass, D. C. *Phys. Rep.* **1980**, *63*, 61.
- (29) Ando, I. *Solid NMR of Polymers*; Saiendefuku: Tokyo, 1994 (in Japanese).
- (30) Kwak, S.-Y.; Nakajima, N. *Macromolecules* **1996**, *29*, 3521.

MA951865D